16th World Conference on Earthquake Engineering, 16WCEE 2017
Santiago Chile, January 9th to 13th 2017
Paper N° 4132 (Abstract ID)
Registration Code: S-XXXXXXXX

SEISMIC ANALYSIS OF RC STRUCTURES WITH ABSENCE OF FLOOR SLAB CONSTRAINTS AND A NON-CONVENTIONAL TMD

R. Ding[(1)], M. X. Tao[(2)], M. Zhou[(3)], J. G. Nie[(4)]

[(1)] *Postdoctoral Scholar, Department of Civil Engineering, Tsinghua University, dingran1988@163.com*
[(2)] *Assistant Professor, Beijing Engineering Research Center of Steel and Concrete Composite Structures, Department of Civil Engineering, Tsinghua University, taomuxuan@tsinghua.edu.cn*
[(3)] *Former PhD. Candidate, Department of Civil Engineering, Tsinghua University, zhoum07@mails.tsinghua.edu.cn*
[(4)] *Professor, Key Lab. of Civil Engineering Safety and Durability of China Education Ministry, Department of Civil Engineering, Tsinghua University, niejg@tsinghua.edu.cn*

Abstract

A case study is presented to reveal the influence of absence of floor slab constraints and large mass turbine as a non-conventional tuned mass damper (TMD) on the seismic behavior of the reinforced concrete (RC) structures and members. The investigated structure is a RC shear wall-frame power plant structure with large slab openings and a large mass turbine. In RC structures, the existence of floor slabs can usually provide strong constraints on beams so as to greatly increase their bearing capacity. However, due to some special functional demands, large area of slabs may have to be removed so that some floor beams will lose the constraints provided by slabs. In such cases, beams could be subjected to complex internal forces and develop unexpected failure modes under earthquake actions. Nonlinear time history analyses are conducted using the self-developed program COMPONA-MARC Version 1.0. The numerical model employs fiber beam-column elements with distributed plasticity approach. The complex seismic behaviors of structural members without slab constraints are elaborately simulated and analyzed. The time history analysis results indicate that for the structural members without slab constraints, significant transverse vibration and large transverse bending moment are the essential factors causing the failure of these components and should be considered with special attention in design. For the seismic effectiveness of the turbine as a TMD with large mass ratio, the optimizing approach is discussed and optimized parameters are verified by extensive numerical examples under a wide selection of ground acceleration time histories.

Keywords: Seismic behavior; Large slab opening; Damage mechanism; Non-conventional TMD; Time history analysis

1. Introduction

In conventional building structures, floor and roof systems are designed at each story to carry the vertical dead and live loads, and to transfer them to beams, columns and walls. For reinforced concrete (RC) structures, the floor slabs are usually cast together with beams, thus providing strong constraints for them and greatly increasing their bending capacities in both flexural directions of the section. In past studies, the effective slab width was proposed and widely investigated to quantitatively reveal the contribution of slabs to the longitudinal bending capacity of the beams [1]. However, to satisfy various functional requirements, a number of special buildings have been designed and constructed with large area of slabs eliminated. Al Harash [2] specially emphasized the effects of slab openings on the structural seismic behavior based on a comprehensive numerical study involving different opening sizes (none, 11%, 15% and 22% of total floor area), but the opening ratio investigated in his study was relatively small and floor slabs still provided strong support to the beams. If the openings ratios reach up to 50%-100%, lots of beams may lose the slab constraints. In such cases, the beams can be subjected to complex internal forces and develop unexpected failure modes. Thus, the effect of large slab openings on the seismic performance of the structure and members should be intensively studied in particular. However, investigations on such critical effect and corresponding special design considerations have rarely been reported in the literature.

On the other hand, to satisfy the structural or architectural functions, auxiliary facilities elastically connected to the floors are often needed. Sometimes the facility mass to structure mass ratio (also referred to as the mass ratio) is very large, and then the facility acts as a non-conventional tuned mass damper (TMD), which has been proposed in recent studies as a new configuration [3-5]. The non-conventional TMD is found to be more robust against off-optimum deviations which could cause a significant reduction of the seismic effectiveness of the conventional TMD [6]. In recent studies, many optimizing approaches have been presented for the TMD [7-10], among which the simple optimizing formula proposed by Tsai and Lin [9] has been verified to be valid for the seismic effectiveness of the conventional TMD by Rakicevic et al. [11]. However, whether this approach is valid for the non-conventional TMD is still not clear.

In this paper, the seismic performance of a RC shear wall-frame power plant structure is investigated by conducting elaborate three-dimensional (3D) elasto-plastic time history analyses and the following two issues are paid attention to: (1) to intensively investigate the influence of the absence of slab constraints on the seismic behavior of corresponding structural members; (2) to discuss the effectiveness of the formula suggested by Tsai and Lin [9] in optimizing the parameters of the turbine as a non-conventional TMD. Nonlinear time history analyses are conducted by using the self-developed nonlinear structural analysis program *COMPONA-MARC Version 1.0* [12]. The numerical model using fiber beam-column elements with distributed plasticity approach can elaborately simulate the complex seismic behavior of structural members without floor slab constraints.

2. Structural system of the investigated building

The investigated building is a twelve-story RC power plant building with 80m height, 24m width and 90m length. The structural system consists of frames with structural shear walls at the lower ten stories, and frames with steel braces at the upper two stories. Fig.1 describes the layout of the columns, beams, walls, braces and slabs at typical floors. The structure's plan is nine 10m bays in length (i.e., in the x-direction) and two 12m bays in depth (i.e., in the y-direction). The story height varies within a wide range from 3m to 10m. Seven shear walls are located asymmetrically at the lower ten stories and six pairs of steel braces are placed at the upper two stories in the x-direction to enhance the lateral stiffness in the corresponding direction.

As can be observed from Fig.1, all the stories except for the roof have different slab openings with ratios ranging from 11% to 100%, among which the ninth and eleventh stories stand out with no slabs (see Figs.1b and 1d) and the latter one even without columns and beams inside (see Fig.1d). It can also be found that slabs are eliminated at all stories within the area from the axis 1 to 3 and A to B except for the roof. Due to the special functions of the plant building, some floors are designed to carry very large loads. A 5600-ton coal scuttle and a 1200-ton high pressure heater stay at the fifth and the seventh floor, respectively. In addition, a 6000-ton turbine

is connected elastically to the ninth floor. The slab thicknesses for the floor and the roof are 100mm and 80mm, respectively.

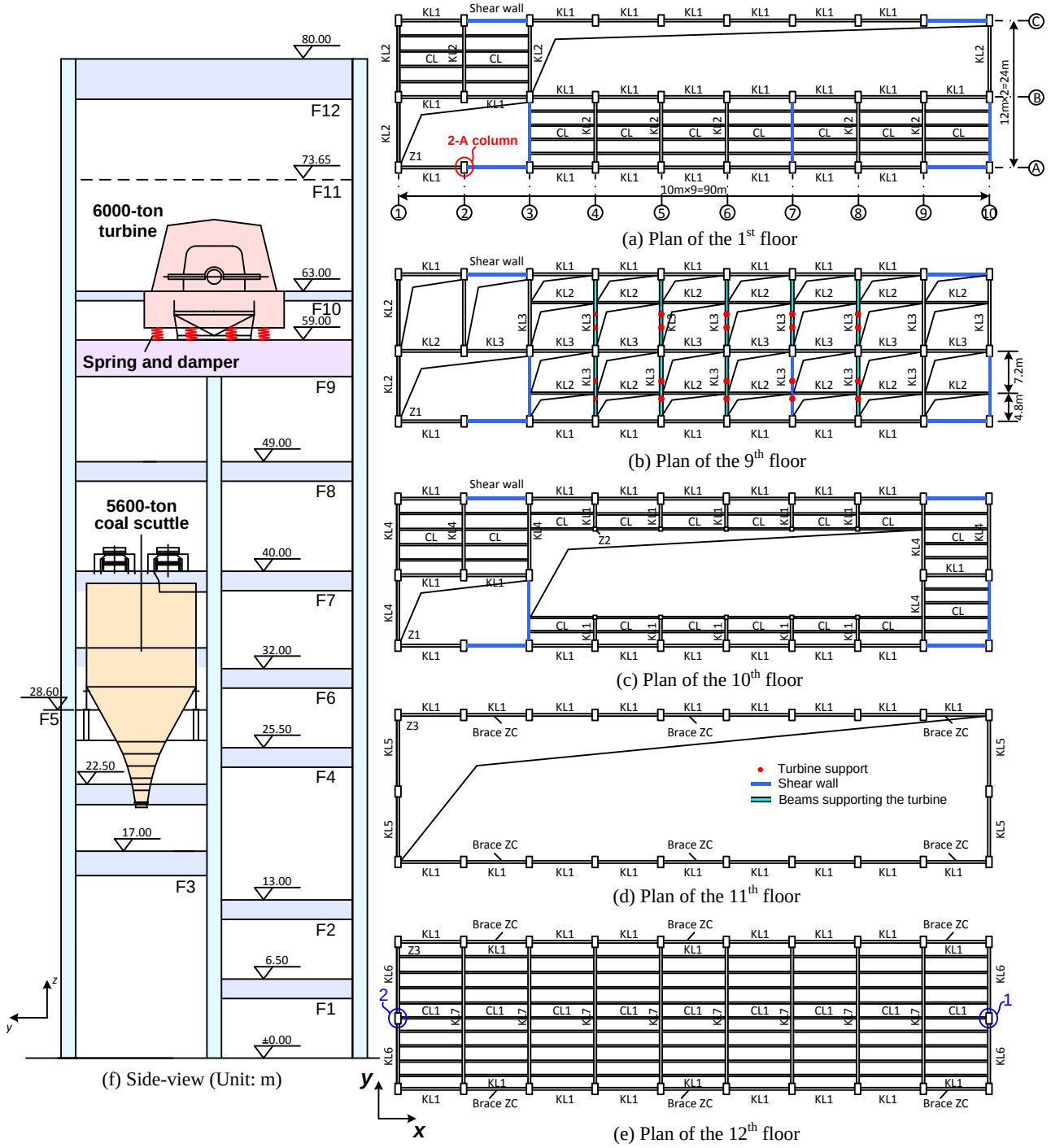

(a) Plan of the 1st floor

(b) Plan of the 9th floor

(c) Plan of the 10th floor

(d) Plan of the 11th floor

(e) Plan of the 12th floor

(f) Side-view (Unit: m)

Fig. 1-Plans and elevation of the structure

Because of the irregular large slab openings, some structural members will lose the slab constraints under earthquakes. Therefore, complex combined internal forces leading to unexpected failure modes of these members may be observed and should be studied carefully. Furthermore, since the mass ratio is around 16%, the turbine-structure interaction may be critical and the turbine can be regarded as a non-conventional TMD. Thus, the investigation on the seismic performance of this power plant building can provide important and valuable

information on the effects of the absence of slab constraints and the large mass turbine as a non-conventional TMD.

3. Numerical modeling

The frame columns and beams are modeled with self-developed fiber beam-column elements [12], which use a displacement-based distributed plasticity approach. The multi-layer shell element proposed by Lu et al. [13] is implemented to model the behavior of shear walls. The adopted uniaxial stress-strain relationship of the concrete material in the fiber beam-column elements is developed by Tao and Nie [12]. The concrete model can accurately trace the actual complex nonlinear seismic behavior of the concrete material in the actual structural members. The constitutive model for steel and reinforcement implemented can accurately consider the Bauschinger effect. The main merit of the adopted beam-column element is that it can predict the potential plastic hinges at any position of the beam or column compared to the practical lumped plasticity approach. The elasto-plastic constitutive model using the von Mises yield surface and the isotropic hardening rule is employed to the concrete in multi-layer shell elements. The smeared crack model is applied to simulate the cracking behavior of the wall concrete. The reinforcement in the multi-layer shell elements is modeled with an orthotropic material using the von Mises yield surface and the kinematic hardening rule. The nodes at the bottom of the column and shear wall are fixed with all degree of freedoms except the two horizontal degree of freedoms which are used as earthquake acceleration input.

Considering that the beams and columns without the constraints of floor diaphragms are the main focuses in this study, the local rigid floor assumption is thus employed to the local areas where slabs remain to simplify the modeling procedure and to enhance the numerical efficiency, while not affecting the analysis results of local structural members. The story mass is computed as 100% of the dead load plus 50% of the live load. The concentrated masses at the fifth and seventh floor are attached to the corresponding supporting beams.

As is mentioned above, the mass of the turbine located at the ninth floor is very large and the turbine supported by twenty bearings covers a large area of about 600m^2. Therefore, the interaction between the turbine and main structure may be complicated and should be considered elaborately. As shown in Fig.2, the turbine is simulated using twenty nodes connected by stiff bars in plane and each node is attached by 300-ton mass. All the twenty nodes are supported elastically with dampers by the floor beams. The elastic supporting system between the turbine and beams is modeled by twenty springs with stiffness and damping in both the *x*- and *y*-directions. The stiffness per spring *k* is 50kN/mm, and the equivalent damping coefficient *c* for each spring is calculated as:

$$c = 2\xi\sqrt{k \cdot m} \tag{1}$$

where *m* is the mass per node; and ξ is the damping ratio, selected as 2%.

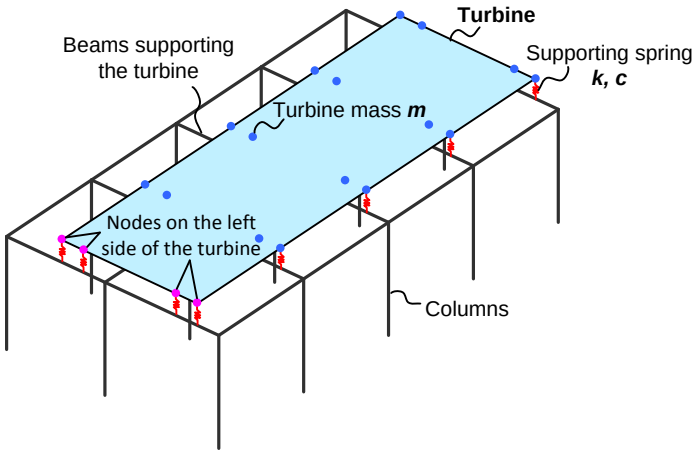

Fig. 2-Turbine-structure interaction model

4. Nonlinear time history analysis results

4.1 Ground motions

Three ground motions including two recorded accelerograms and one artificial accelerogram are chosen as inputs in the present time history analysis. The two recorded accelerograms are gained at the El-Centro station in the USA in 1940 and the Taft station in the USA in 1952, respectively. The artificial accelerogram is generated to match the elastic response spectra stipulated by the *Chinese Code for Seismic Design of Buildings* (CCSDB) [14]. In a routine seismic design based on the CCSDB [14], a structure should meet the performance requirements at two different earthquake levels specified by the probability of occurrence. At the first level, elastic response without significant structural damage is required under the frequent earthquake which is defined as the earthquake with the 50-year exceedance probability equal to 63%, and at the second level, no collapse is required under the severe earthquake which is defined as the earthquake with the 50-year exceedance probability equal to 2%. In order to satisfy the above two performance requirements, the peak ground accelerations (PGAs) of the selected motions are scaled to 550 mm/s^2 and 3100 mm/s^2, respectively, as stipulated in CCSDB [14] for the earthquake intensity of 7.5.

Additionally, the natural ground motion input is applied in both the *x*- and *y*-directions of the structure at the same time using the two recorded horizontal orthogonal components. Since the artificial accelerogram contains only one horizontal component, it is applied in the *x*- and *y*- directions simultaneously using the same accelerogram with the PGA ratio of the two directions as 1:0.85. The primary input direction is chosen as *x* and *y* respectively and thus totally 12 cases are calculated. The damping ratio is chosen as 5%, which is usual for RC structures.

4.2 Analysis of the results

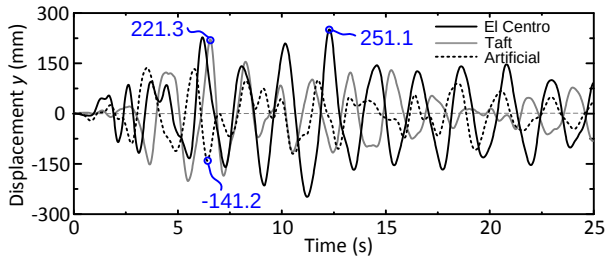

(a) Average roof displacements *y*

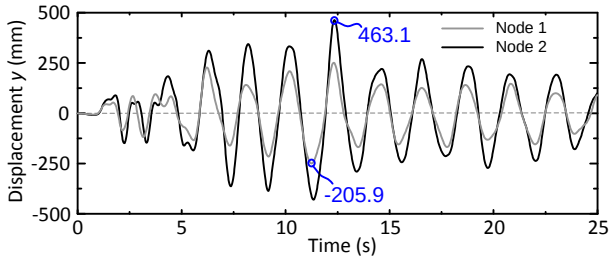

(b) Roof displacements *y* for nodes 1 and 2 (El Centro)

Fig. 3-Roof displacement responses under severe earthquake with main direction y

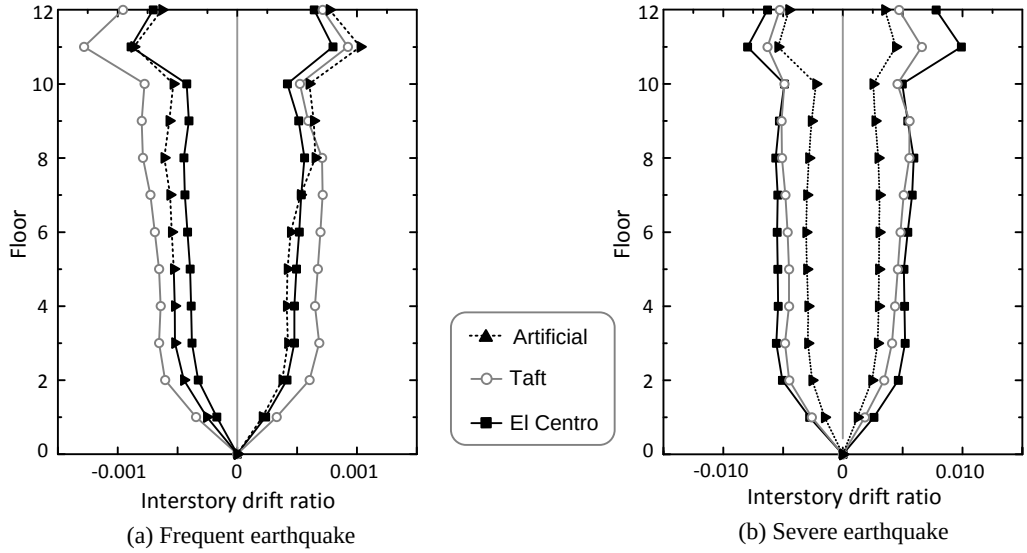

(a) Frequent earthquake (b) Severe earthquake

Fig. 4-Interstory drift ratio envelops under earthquakes with main direction y

4.2.1 Roof displacement and interstory drift

The average roof displacements of the structure under severe earthquakes with main direction *y* are shown in Fig.3a. The largest displacement response occurs under the excitation of El Centro record. In addition, the roof displacements at nodes 1 and 2 as shown in Fig.1e are plotted together in Fig.3b. Significant difference of the displacements between nodes 1 and 2 can be found, indicating an evident torsional effect of the structure.

The envelope curves of interstory drift ratio in the *y*-direction are plotted in Fig.4. The figure reveals that for the frequent and severe earthquake, the largest interstory deformation is caused by the Taft and El Centro records, respectively. Due to the lack of the floor slabs, middle columns and *y*-direction shear walls or braces, the eleventh story becomes the weakest story leading to the largest interstory drift ratio among all the stories. The maximum drift ratios under frequent and severe earthquakes are 1/781 and 1/101, which are smaller than the allowable values of 1/550 and 1/50 stipulated by CCSDB [14], respectively. As a result, the structure satisfies the global deformation limitation requirements of the code provisions at the two different performance levels.

4.2.2 Damage mode analysis of the structure

It is demonstrated from the time history analysis that the structure remains elastic under frequent earthquake. However, under severe earthquake excitation, the structure deforms plastically with many plastic hinges formed on the beams and columns. Fig.5 shows the distributions of plastic hinges at different times under the El Centro record which causes the severest damage with largest interstory drift ratio to the structure. At the 3rd second of the ground motion, it can be seen that plastic hinges mainly form at the ends of beams and columns in the weak story. The ends of the beams connected to the 2-A column are also found to develop plastic hinges which are caused by the local vibration of the column without the slab constraints. Similarly, the transverse vibration of beams supporting the turbine causes plastic hinges at the midspan of the beams and the ends of the columns supported by these beams. After the seismic excitation lasts 6.1 seconds, rebars of the first-story columns begin to yield. When the ground motion comes to the end at the 25th second, plastic hinges develop at the ends of all the beams between the three columns at the 1-axis. The bottom ends of some first-story columns at the 2-axis and 3-axis also yield. This may be explained that the torsional effect of the whole structure due to the asymmetrical layout of shear walls and irregular slab openings results in more pronounced displacement response of these three frames located at the end of the structural plane. In addition, as shown in Fig.5c, the beam at the ninth floor connecting the beam supporting the turbine to the shear wall develops full-length plastic

hinges, which is resulted from the large tensile force caused by the transverse vibration of the beam supporting the turbine.

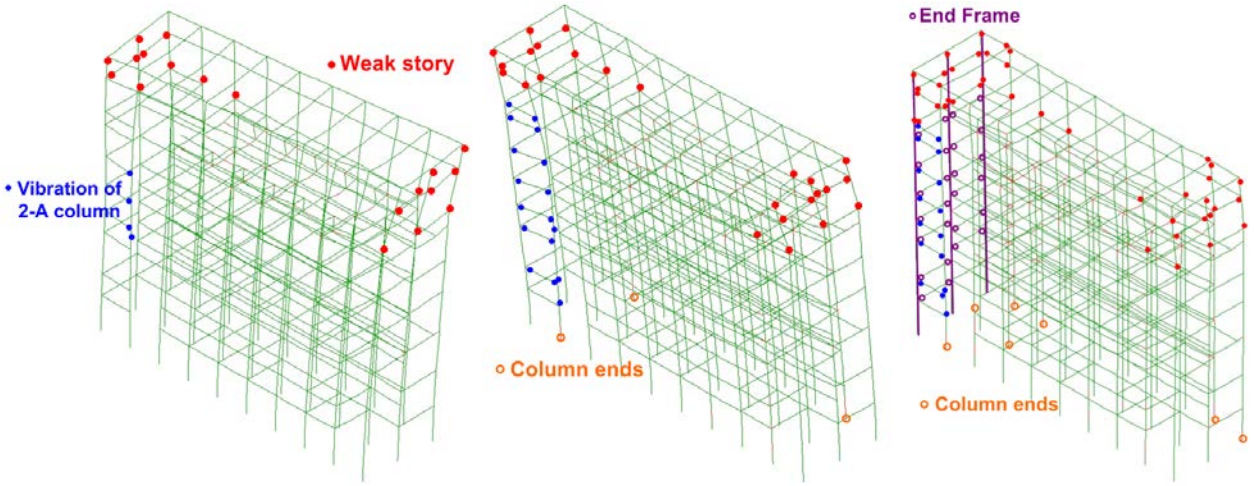

(a) t = 3s (b) t = 6.1s (c) t = 25s

Fig. 5-Distribution and development of plastic hinges under the El Centro record

4.2.3 Damage mechanism analysis of structural members

The analysis of damage mode of the structure under severe earthquakes reveals that some local structural members suffer unexpected damage. The internal forces and damage mechanisms of these members will be discussed in detail here, and suggestions for optimizing the design will also be proposed.

As shown in Figs.6a and 6b, two beams with the same span, cross-sectional dimension and reinforcement arrangement are compared in terms of internal forces and reinforcement stress to illustrate the influence of the large slab openings. One beam is at the sixth floor between the 1-A and 2-A columns (referred to as beam 1 hereinafter) without the lateral constraints provided by floor diaphragms and frame beams in its perpendicular direction. The other beam is at the eighth floor between the 8-A and 9-A columns (referred to as beam 2 hereinafter) with the constraints provided by floor slabs and perpendicular frame beams. Under the severe earthquake of the El Centro record with main direction *y*, plastic hinges appear in beam 1 while no plastic hinges are found in beam 2.

In order to reveal the damage mechanisms of these two beams, the internal forces at the A-A section of beam 1 and B-B section of beam 2 are calculated and compared. It can be seen from Figs.6c and 6d that the longitudinal bending moment of beam 1 is less than that of beam 2 while the transverse bending moment of the former one is about four times larger than that of the latter one, which is very unusual. Since the longitudinal moment for the two beams are both smaller than the corresponding bending capacity, the plastic hinge of beam 1 is surely induced by the significant transverse bending moment. This will be verified by the stress response of rebar A which lies near the middle part of the beam section (see Fig.6g) as shown in Fig.6e. The maximum tensile stresses of rebar A in beams 1 and 2 are 335MPa and 90MPa, respectively, indicating that a transverse bending plastic hinge only forms at the ends of beam 1. Therefore it can be concluded that the plastic hinge is caused by the insufficient transverse bending capacity of beam 1 with a narrow section.

Generally speaking, without floor slab openings, the transverse bending moment of frame beams is small and negligible. However, as shown in Fig.1, due to the removal of slabs surrounded by the axes 1, 3, A and B, and the frame beams between the 2-A and 2-B columns, the 2-A column in this building structure suffers evident transverse vibration. This will result in the transverse vibration of beam 1 connected to the 2-A column and thus the large transverse bending moment at the ends. Besides, large torsional moment can also be observed in beam

1 as shown in Fig.6f. So it is concluded that beam 1 is a component subjected to complex loading conditions of combined bi-directional bending moments, torsion and shear.

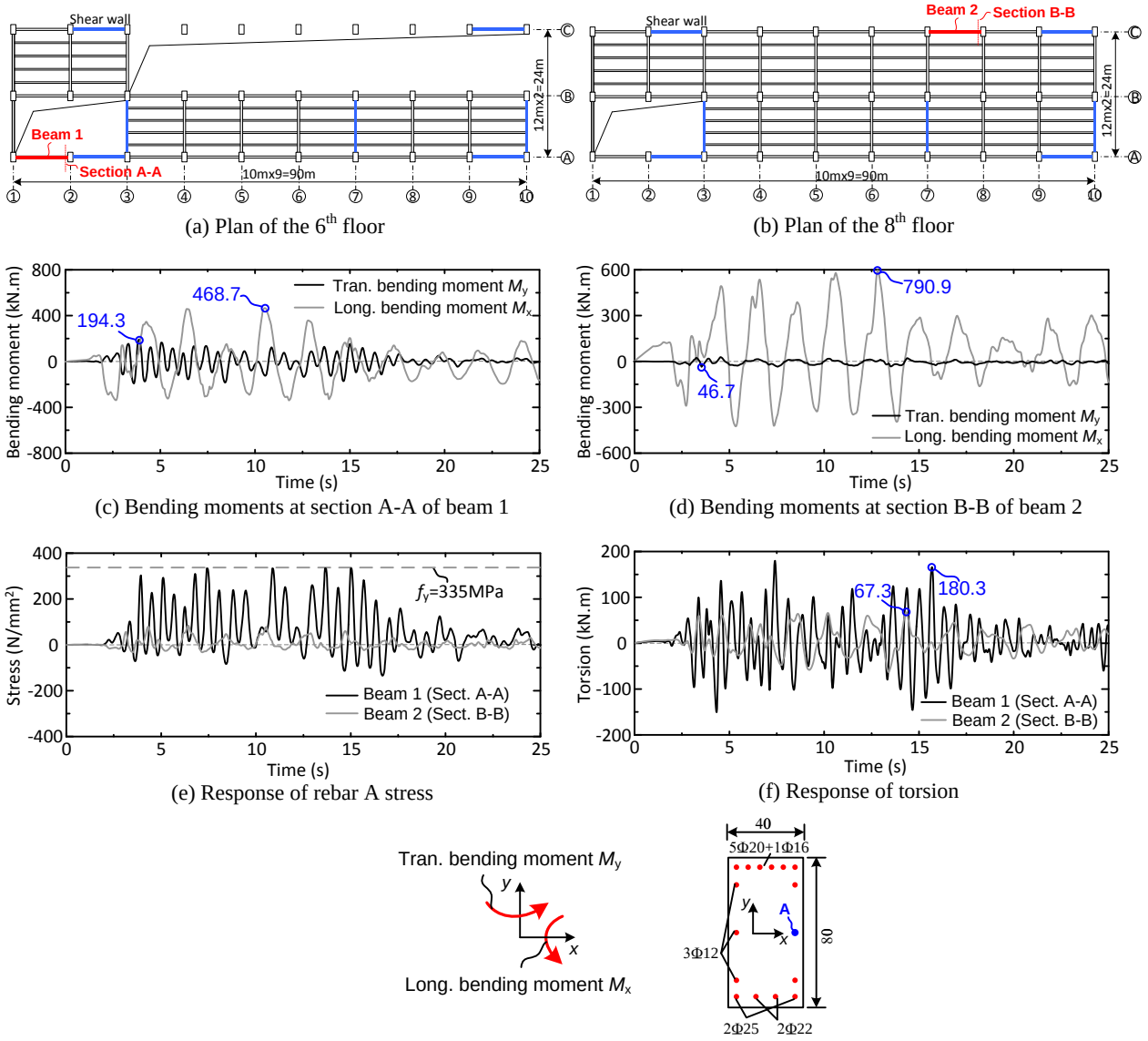

(a) Plan of the 6th floor

(b) Plan of the 8th floor

(c) Bending moments at section A-A of beam 1

(d) Bending moments at section B-B of beam 2

(e) Response of rebar A stress

(f) Response of torsion

(g) Sections of beam 1 and beam 2

Fig. 6-Comparison of structural members with and without slab constraints

It can be drawn from the damage mechanism analysis of these special components without slab constraints that significant transverse vibration of these members can not be ignored. The vibration causes large transverse bending moment and even large torsional moment. The complex combination of different internal force components dominates the failure modes of these special structural members, which should be considered with special attention in design. As a result, these member sections must be widened and additional rebar on the left and right sides of the sections is proposed to enhance the transverse flexural stiffness and strength.

It should also be noted that, in common seismic design and practical time history analysis, beam-column elements with lumped plasticity hinges are preferred and widely used for its simplicity and efficiency. In this kind of element, it is assumed that the plasticity hinges appear at the two ends and the element between the plasticity hinges behaves elastically. However, in this paper, plastic hinges appear at the mid-span of the beams due to the absence of slab constraints. If lumped plasticity model is employed, this important and special damage

mode will not be captured, causing unsafe design for these beams. So it is recommended that for structures with large slab openings, distributed plasticity approach should be applied.

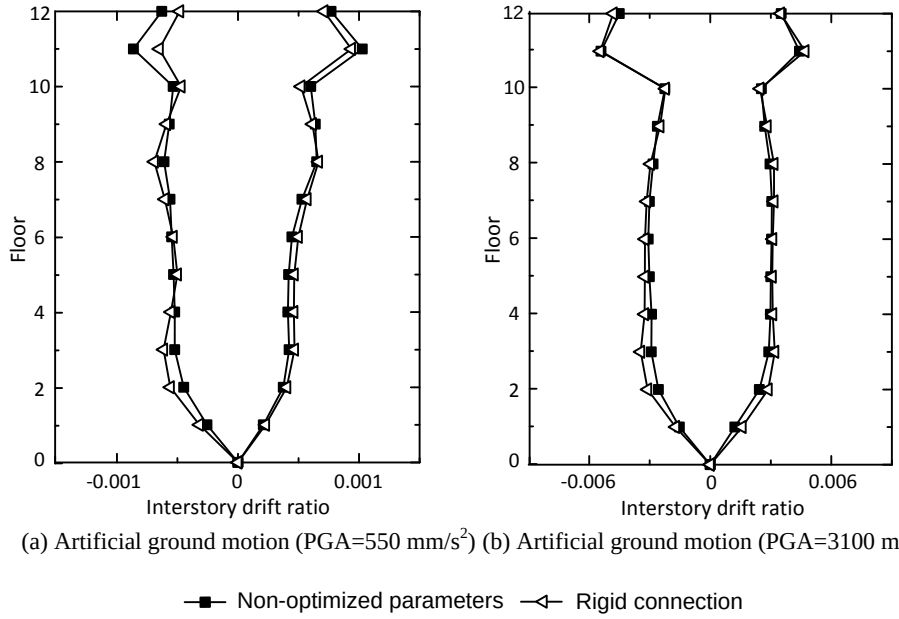

(a) Artificial ground motion (PGA=550 mm/s^2) (b) Artificial ground motion (PGA=3100 mm/s^2)

Fig. 7-Comparison of interstory drift ratio envelops between models with non-optimized turbine parameters and turbine rigidly connected to the structure

5. Optimization of the turbine as a non-conventional TMD

5.1 Seismic effectiveness of original non-optimized parameters

In the investigated building structure, the 6000-ton turbine elastically connected to the floors can be considered as a non-conventional TMD for the main structure. The seismic effectiveness of the TMD with original non-optimized parameters is firstly estimated to determine whether the optimization is needed. The effectiveness should be evaluated through the comparison between the controlled configuration (turbine as a TMD) and the uncontrolled configuration (turbine rigidly connected to the structure). The main direction of ground motion input is chosen as *y* since the structural response is larger in this case. Thereby, the 6 cases in the time history analysis conducted in Section 4 are re-calculated with the turbine rigidly connected to the structure.

Some typical comparison between the deformation response results of the controlled and uncontrolled configuration is illustrated in Figs.7 as well as Table 1. It is found that the TMD with original non-optimized parameters is invalid and even amplify the response of the main structure under the excitation of severe El Centro record, frequent Taft record and frequent artificial ground motion. Thereby the effectiveness is quite unsatisfactory and it is necessary to suggest better parameters for the TMD to ensure its seismic effectiveness.

5.2 Discussion and verification of the optimized parameters

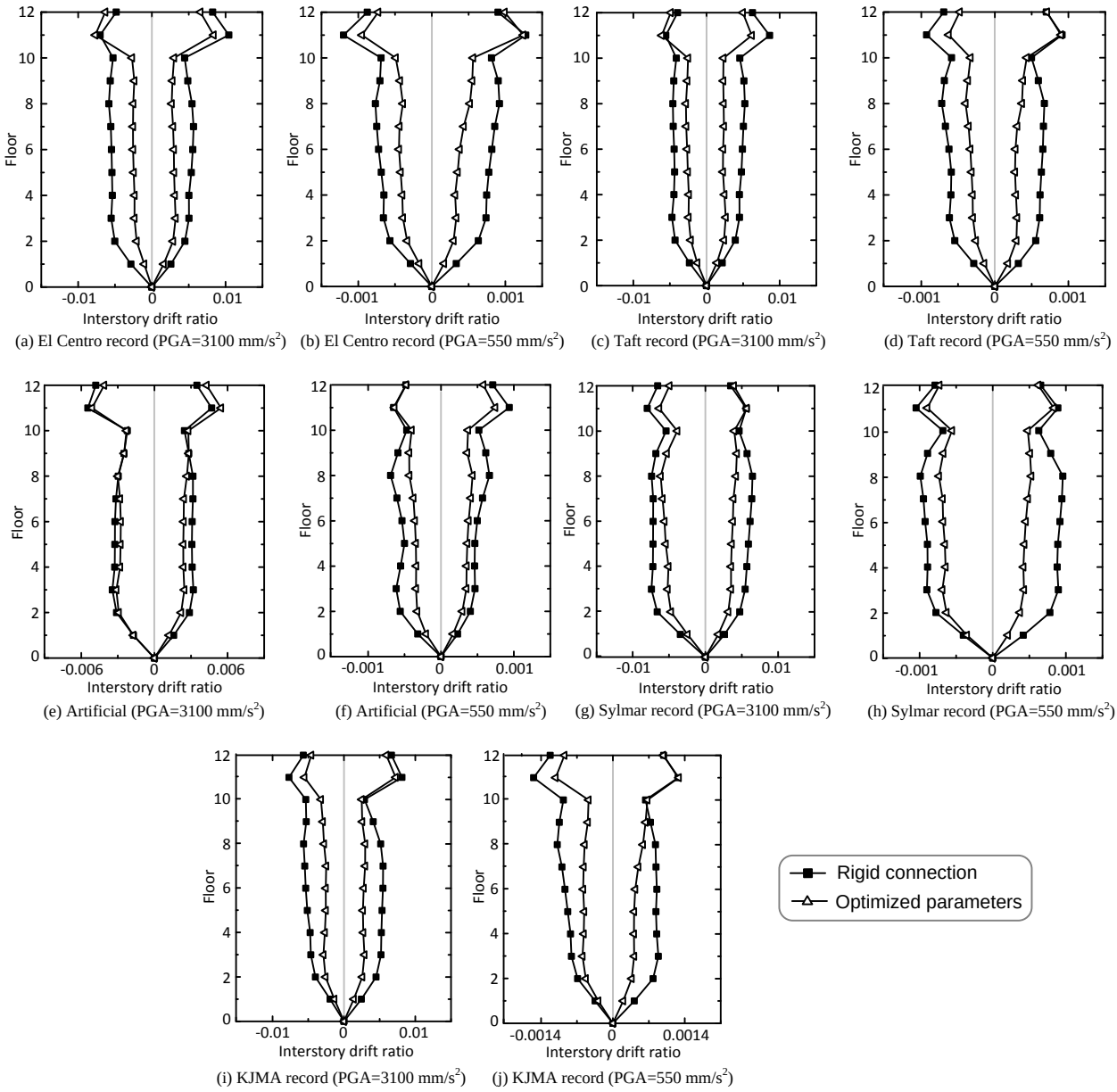

Fig. 8-Comparison of interstory drift ratio envelops between models with optimized turbine parameters and turbine rigidly connected to the structure

The TMD is optimized according to Eq. (2) proposed by Tsai and Lin [9] including natural damping of the structure.

$$f = \left(\frac{\sqrt{1-0.5\gamma}}{1+\gamma} + \sqrt{1-2\xi_p^2} - 1 \right) - (2.375 - 1.034\sqrt{\gamma} - 0.426\gamma)\sqrt{\gamma}\xi_p - (3.730 - 16.903\sqrt{\gamma} + 20.496\gamma)\sqrt{\gamma}\xi_p^2$$

$$\xi_s = \sqrt{\frac{3\gamma}{8(1+\gamma)(1-0.5\gamma)}} + (0.151\xi_p - 0.170\xi_p^2) + (0.163\xi_p + 4.980\xi_p^2)\gamma \quad (2)$$

where f is the optimum ratio of the TMD natural frequency to the first natural frequency of the main structure; γ is the damper mass to main structure mass ratio; ξ_p is the damping ratio of the main structure; and ξ_s is the optimum damping ratio of the damper.

The calculated optimum frequency ratio f and damping ratio ξ_s of the TMD according to Eq. (2) for the investigated building are 0.787 and 0.247, respectively. Then time history analyses are then performed using these two optimized parameters under a wide selection of ground acceleration time histories, both natural and artificial, so that the influence of frequency content on the effectiveness of the proposed large mass ratio TMD could be assessed. In detail, the selected time histories include an artificial accelerogram as used before, and four natural accelerograms, selected from *Strong Ground Motion Database* [15]. Among them, records from Northridge (Sylmar, 1995) and Kobe (KJMA, 1994) earthquakes are characterized by long-period pulse-like waveforms, and thus they are typically classified as near-fault ground motions. Records from Imperial Valley (El Centro, 1940) and Kern County (Taft, 1952) earthquakes have instead fewer long-period characteristics, so they are used to represent far-field ground motions.

Table 1-Comparison of maximum interstory drift ratios between models with non-optimized turbine parameters and turbine rigidly connected to the structure

Ground motion		Maximum interstory drift ratio		
		Rigid connection	Non-optimized parameters	Amplification / Reduction
Frequent	El Centro	1/783	1/1126	Reduction
	Taft	**1/1078**	**1/781**	**Amplification**
	Artificial	**1/1068**	**1/974**	**Amplification**
Severe	El Centro	**1/105**	**1/101**	**Amplification**
	Taft	1/116	1/153	Reduction
	Artificial	1/182	1/185	Reduction

Table 2-Comparison of maximum interstory drift ratios between models with optimized turbine parameters and turbine rigidly connected to the structure

Ground motion		Maximum interstory drift ratio		
		Rigid connection	Optimized parameters	Reduction ratio
Frequent	El Centro	1/783	1/804	2.6%
	Taft	1/1078	1/1112	3.1%
	Artificial	1/1068	1/1344	20.5%
	Sylmar	1/955	1/1116	14.4%
	KJMA	1/648	1/779	16.8%
Average		**1/872**	**1/987**	**13.1%**
Severe	El Centro	1/105	1/120	12.5%
	Taft	1/116	1/162	28.4%
	Artificial	1/182	1/183	0.1%
	Sylmar	1/125	1/156	19.9%
	KJMA	1/81	1/92	12.0%
Average		**1/114**	**1/134**	**18.0%**

The two different PGAs of 550 mm/s^2 and 3100 mm/s^2 are analyzed for each ground motion to check the influence of PGA on the seismic effectiveness of TMD and 10 cases in total are thus calculated. Table 2 and Fig.8 show the time history analysis results and it is demonstrated that, in average, the maximum interstory drift ratios for severe earthquakes with 3100-mm/s^2 PGA and frequent earthquakes with 550-mm/s^2 PGA can be reduced by 18.0% and 13.1%, respectively. So it is stated that the formula proposed by Tsai and Lin [9] is quite effective for the non-conventional TMD in the investigated building.

5.3 The seismic response of the turbine with optimized parameters

As an essential aspect of the non-conventional TMD, the turbine should retain its own function in addition to the control function as a TMD. The acceleration responses are mostly concerned in the design of auxiliary facilities such as the turbine under ground motions. Therefore, the acceleration response is taken into account and investigated besides the optimization and evaluation of the seismic effectiveness of the turbine. In addition, the turbine's response is expected to be compatible with possible requirements. As shown in Table 3, the turbine's acceleration responses in all of the 10 cases that are analyzed in Section 5.2 with optimized parameters are obtained and investigated. It is demonstrated that for frequent earthquakes with 550-mm/s^2 PGA, the maximum acceleration of the turbine in the *x*- and *y*- direction are 682.6 mm/s^2 and 430.6 mm/s^2, respectively and for severe earthquakes with 3100-mm/s^2 PGA, the two maximum accelerations are 3030.8 mm/s^2 and 2389.7 mm/s^2, respectively. All the maximum accelerations occur under the excitation of Northridge record. The acceleration requirements for the turbine under frequent and severe earthquakes are 1200 mm/s^2 and 4000 mm/s^2, respectively [16]. Therefore, it is concluded that the turbine's acceleration responses satisfy the corresponding requirements.

Table 3-Maximum accelerations of the turbine in both directions

Ground motion		Maximum acceleration (mm/s^2)	
		x-direction	*y*-direction
Frequent	El Centro	463.5	365.5
	Taft	420.0	404.7
	Artificial	429.0	316.6
	Sylmar	**628.6**	**430.6**
	KJMA	465.6	351.9
Severe	El Centro	2145.1	2135.8
	Taft	2273.6	1699.8
	Artificial	1943.3	1655.6
	Sylmar	**3030.8**	**2389.7**
	KJMA	2699.7	1354.4

6. Conclusions

In this contribution 3D nonlinear time history analyses of a RC shear wall-frame building are conducted as a case study. The building shows some remarkable characteristics such as large slab openings and a turbine with large mass ratio. Therefore it is carefully analyzed to intensively investigate the influence of the absence of floor slab constraints on the seismic behavior of corresponding structural members, and to discuss the seismic effectiveness of the simple formula suggested by Tsai and Lin [9] in optimizing the parameters of the non-conventional TMD. The time history analysis results indicate that for the structural members without slab constraints, significant transverse vibration and large transverse bending moment are not negligible. It is the essential factor causing the failure of these components and should be considered with special attention in design. In addition, the practical lumped plasticity approach commonly used in design cannot capture the complex behavior of these components and may give unsafe predictions. Therefore, a fiber beam-column element with distributed plasticity approach is recommended in modeling such kind of structure. The simple formula suggested by Tsai and Lin [9] is applied to optimize the non-conventional TMD to reduce the dynamic response of the main structure. The effectiveness of this formula for the investigated complex RC structure with relatively high natural damping is verified by extensive numerical examples under a wide selection of ground acceleration time histories. In addition, the turbine's acceleration responses with optimized parameters are found to satisfy the corresponding requirements.

Acknowledgments

The writers gratefully acknowledge the financial support provided by the Beijing Natural Science Foundation (Grant number 8162023) and the National Natural Science Foundation of China (Grant number 51378291).

References

[1] Pantazopoulou S J, French C W (2001) Slab participation in practical earthquake design of reinforced concrete frames. *ACI Strut J*, **98** (4): 479-489.

[2] AL Harash MT (2011) Inelastic seismic response of reinforced concrete buildings with floor diaphragm openings. *Ph.D. thesis*, Washington University in St. Louis, Saint Louis, Missouri, USA.

[3] Feng MQ, Mita A (1995) Vibration control of tall buildings using mega subconfiguration. *ASCE J Eng Mech*, **121** (10): 1082-1088.

[4] Ziyaeifar M, Noguchi T (1998) Partial mass isolation in tall buildings. *Earthq Eng Struct Dyn*, **27** (1):49-65.

[5] Chey MH, Chase JG, Mander JB, Carr AJ (2010) Semi-active tuned mass damper building system: application. *Earthq Eng Struct Dyn*, **39** (1): 69-89.

[6] Angelis MD, Perno S, Reggio A (2012) Dynamic response and optimal design of structures with large mass ratio TMD. *Earthq Eng Struct Dyn*, **41** (1): 41-60.

[7] Den Hartog J P (1956) *Mechanical Vibrations (4th edition)*. McGraw-Hill: New York.

[8] Warburton GB (1982) Optimum absorber parameters for various combinations of response and excitation parameters. *Earthq Eng Struct Dyn*, **10** (3): 381-401.

[9] Tsai HC, Lin GC (1993) Optimum tuned-mass dampers for minimizing steady-state response of support-excited and damped systems. *Earthq Eng Struct Dyn*, **22** (11): 957-973.

[10] Sadek F, Mohraz B, Taylor AW, Chung RM (1997) A method of estimating the parameters of tuned mass dampers for seismic applications. *Earthq Eng Struct Dyn*, **26** (6): 617-635.

[11] Rakicevic ZT, Bogdanovic A, Jurukovski D, Nawrotzki P (2012) Effectiveness of tune mass damper in the reduction of the seismic response of the structure. *Bull Earthquake Eng*, **10** (3): 1049-1073.

[12] Tao MX, Nie JG (2014) Fiber beam-column model considering slab spatial composite effect for non-linear analysis of composite frame systems. *J Struct Eng*, **140** (1): 04013039.

[13] Lu X, Lu XZ, Guan H, Ye LP (2013) Collapse simulation of reinforced concrete high-rise building induced by extreme earthquakes. *Earthq Eng Struct Dyn*, **42** (5): 705-723.

[14] Ministry of Construction of the People's Republic of China (MCPRC) (2010) *Code for seismic design of buildings (GB 50011-2010)*. China Architecture and Buildings Press: Beijing.

[15] Pacific Earthquake Engineering Research Center (PEER) (2013) Strong ground motion database. *http://peer.berkeley.edu/* [10 May 2013]

[16] Yin XJ, Wang WQ, Gu CH, Sha ZX (2012) Re-thinking of seismic protection for equipments at power plants. *Eng J Wuhan Univ*, **45** (S1): 298-301. (in Chinese)